Open Access

Journal of Energy and Power Technology

LIDSEN Publishing Inc.

Original Research

Overall Reaction Rate Study of Thermal Methane Cracking in Non-Isothermal Conditions

Mahdi Yousefi [1, *], Scott Donne [1], Shabnam Bahremand Abrasi [2], Mohammad Yousefi [3]

1. PRC for Frontier Energy Technologies and Utilization, University of Newcastle, Callaghan, NSW 2308, Australia; E-Mails: mahdi.yousefi@uon.edu.au; Scott.Donne@newcastle.edu.au
2. Environmental Remediation (GCER), University of Newcastle, Callaghan, NSW 2308, Australia; E-Mail: Shabnam.Bahremandabrasi@uon.edu.au
3. Tehran Azad University of University Science and Research, Chemical Engineering Department, Ferdos Blvd, Tehran, Iran; E-Mail: mmyousefi94@gmail.com

* **Correspondence:** Mahdi Yousefi; E-Mail: mahdi.yousefi@uon.edu.au

Academic Editors: Zhiwei Ma and Huashan Bao

Special Issue: Decarbonisation of Heating and Cooling

Journal of Energy and Power Technology
2023, volume 5, issue 3
doi:10.21926/jept.2303028

Received: April 10, 2023
Accepted: September 07, 2023
Published: September 13, 2023

Abstract

The thermal cracking of methane (TMC) is a significant reaction occurring above 850°C, which proceeds in two stages: non-isothermally and isothermally. However, most existing studies have focused on obtaining reaction rates under isothermal conditions [1], limiting their applicability to practical industrial reactor conditions. This novel research aims to determine the overall thermal decomposition rate of methane to hydrogen and carbon in adiabatic conditions, covering the range of unstable industrial reactor temperatures (850 to 1200°C). The Coats and Redfern model-fitting method was employed to calculate the reaction rate under non-isothermal conditions, and the resulting models were compared with experimental data. The findings reveal the Contracting Cylinder model as the best-fit mathematical representation with less than ±2.8% error. By extending the kinetic model to non-isothermal conditions, this approach addresses a critical aspect of real-world applications.

© 2023 by the author. This is an open access article distributed under the conditions of the Creative Commons by Attribution License, which permits unrestricted use, distribution, and reproduction in any medium or format, provided the original work is correctly cited.

Keywords
Thermal methane cracking; hydrogen production; overall reaction rate; adiabatic conditions

1. Introduction

Thermal cracking of natural gas is a promising process for simultaneous hydrogen production and distribution [1]. In this process, pure hydrogen is obtained from the thermal decomposition of natural gas. The availability of natural gas in many regions, as well as the possibility of producing very pure hydrogen without advanced purification systems, make it an attractive option. It could eliminate the need for extensive hydrogen transportation and storage, which are major obstacles to developing hydrogen applications [1-3].

However, thermal methane cracking is still an immature technology for industrial and semi-industrial scales, and more research is needed to understand all the advantages and challenges. Among these challenges is obtaining an accurate examination of the overall reaction rate at all temperature intervals. Despite numerous investigations, an exact characterisation of the cracking reaction has not been achieved [4]. Although methane is the simplest hydrocarbon, the mechanisms of its decomposition reactions are not fully understood, and precise characterisation of the mechanisms has not been reported [5-7]. In their study, Mahdi et al. [4] provided an overview of the sub-reactions involved in the thermal methane cracking process (Figure 1) and the different species that contribute to the cracking reactions from the reactant CH_4 to the final products (H_2 and C).

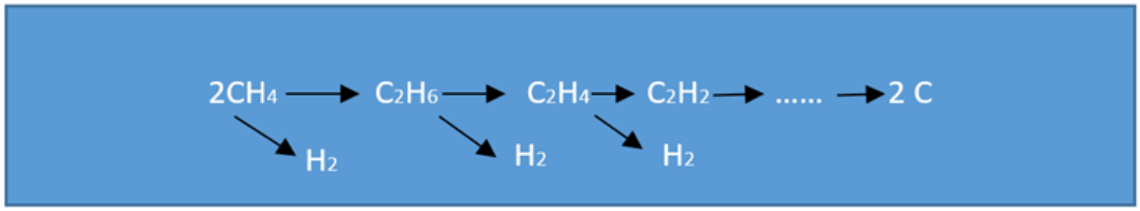

Figure 1 Thermal methane cracking kinetic model shows the intermediates products in MTC immediately converted to hydrogen and carbon and are on the path from the reactant (methane) to the final products [4].

Previous studies have mainly focused on the mechanism of intermediate reactions and materials, leading to general mass transfer coefficient (MTC) reaction rates that are only valid for isothermal conditions. For example, Wullenkord et al. [8] tried to investigate the conversion rate of methane at 1200 to 1600°C. It should be noted that the thermal decomposition reaction of methane above 850°C is significant and cannot be ignored and should be considered when methane is heated up in a non-isothermal condition. It is also well-confirmed with other published studies, such as Lee et al. [9] and Trommer et al. [10] conducted for temperatures lower than 850°C. Holmen et al. [7] described a model for the production and consumption of the main hydrocarbons at both high and low conversion rates of CH_4 in the temperature range of 1196-1450°C, and the results of the experimental tests and the model predictions were almost close.

However, it could not cover lower temperature rates as the method was based on an isothermal condition. The nature of most industrial reactors is such that the gas temperature varies throughout the reactor, and the reaction occurs when the feed gas is warming up inside the reactor. Thus, it is necessary to obtain an overall reaction rate covering both non-isothermal and isothermal stages to model an unstable reactor. This research aims to study the overall reaction rate of thermal decomposition of methane in the 850 to 1200°C temperature range in adiabatic conditions using a model-fitting method and to compare the results with experimental data obtained using COMSOL Multiphysics software [4].

2. Background

This study is based on experimental data obtained by the authors and recently published in the Frontiers in Energy Research Journal (2022) [4]. The study aimed to convert methane into hydrogen and methane using a tubular reactor filled with inert ceramic packings under isothermal conditions in the temperature range of 850 to 1200°C. According to Table 1, which shows the concentration of hydrogen at 850 to 1170°C obtained in the experiments, the reaction rate at temperatures lower than 850°C is very slow, indicating negligible conversion of methane during the heating up process. However, at higher temperatures, the cracking reaction is significant, and the reaction can be divided into isothermal and non-isothermal steps as the temperature of the methane gas increases.

Table 1 the concentration of hydrogen at the reactor outlet at 850 to 1170°C and 0.2 to 2 l/min methane feed rate [4].

Methane feed rate (l/min)	Hydrogen percentage (%w/w)							
	850°C	900°C	950°C	1000°C	1050°C	1100°C	1150°C	1170°C
0.20	29.21	47.56	67.4	79.56	90.11	96.66	97.86	99.111
0.40	20.12	41.25	62.25	78.17	88.27	95.87	97.97	99.43
0.60	11.71	37.24	56.53	75.63	87.36	94.72	97.59	99.36
0.80	10.99	36.61	53.34	72.62	85.98	93.51	97.44	99.12
1.00	9.82	29.01	46.25	72.29	82.07	93.03	97.68	99.02
1.20	7.75	24.31	42.6	70.39	80.91	91.13	98	98.24
1.40	7.431	21.55	39.76	67.76	79.35	90.92	96.39	97.75
1.60	6.05	20.63	37.89	63.58	76.03	89.64	95.14	96.29
1.80	3.93	19.1	36.62	61.74	74.61	84.82	94.17	95.92
2.00	3.42	17.47	34.89	60.03	73.91	82.02	93.16	94.13

2.1 Non-Isothermal Reaction Rate Models Description

The non-isothermal reaction rate model can be described using Equation (1), which gives the overall reaction rate as a function of time, temperature, and the temperature-dependent kinetic constant. The degree of conversion at any time is calculated using Equation (2). Equation (3) provides a way to define Equation (1) in terms of the reaction rate constant and the integral model

of the reaction. Table 2 lists some of the common mathematical integral models used for non-isothermal reaction rates, based on different f(α) and g(α).

Table 2 The common mathematical integral models for non-isothermal reaction rates models [11, 12].

	Reaction Model	*f(α)*	*g(α)*
1	Diffusion control (Crank)	$3/2[(1-\alpha)^{-\frac{1}{3}}-1]^{-1}$	$1-\frac{2}{3}\alpha-(1-\alpha)^{\frac{2}{3}}$
2	Diffusion control (Janders)	$2(1-\alpha)^{2/3}[1-(1-\alpha)^{1/3}]-1$	$[1-(1-\alpha)^{1/3}]^2$
3	One dimensional Diffusion	$1/2\ \alpha^{-1}$	α^2
4	Contracting Sphere	$3(1-\alpha)^{2/3}$	$1-(1-\alpha)^{1.3}$
5	Contracting cylinder	$2(1-\alpha)^{0.5}$	$1-(1-\alpha)^{0.5}$
6	Mampel (first order)	$1-\alpha$	$-\ln(1-\alpha)$
7	Second Order	$(1-\alpha)^2$	$(1-\alpha)^{-1}-1$
8	Avrami-Erofeev	$3(1-\alpha)[-\ln(1-\alpha)]^{2/3}$	$[-\ln(1-\alpha)]^{1/3}$

Under non-isothermal reaction conditions, the kinetic constant k(T) can be described by the Arnious equation. Equations (4) and (5) explain Equations (1) and (3), respectively, in terms of the kinetic constant and the heating rate (β = dT/dt). Equation (6) is the integration of Equations (4) and (5), and it can be rewritten as Equation (7) by considering x = E/RT, where L(x) is an exponential integral that does not have an analytical solution but can be estimated numerically.

There are two main non-isothermal approaches to obtaining the kinetic parameters: model-fitting and model-free methods. The model-fitting method involves fitting different models to α vs temperature curves and defining E and A parameters concurrently. The Coats and Redfern method is one of the most common models for model-fitting methods and uses an asymptotic series expansion, as shown in Equation (9), where T^m is the mean temperature.

Equation (1) is a mathematical model to describe overall non-isothermal reaction rates:

$$\frac{d\alpha}{dt} = k(T) \times f(\alpha) \tag{1}$$

$$\alpha = \frac{m_0 - m_t}{m_0 - m_f} \tag{2}$$

α is the degree of conversion at any time calculated by equation (2), t is the time, T is temperature, k(T) is the temperature-dependent kinetic constant, f(α) is the reaction model, which is an empirical function to express the change in the reactivity as the reactions proceed (dimensionless). m_0 is the initial mass of the sample and m_t is the time-dependent mass. m_f is the final mass of the sample.

Equation (1), which describes the overall non-isothermal reaction rate (dα/dt), can be related to Equation (3) as follows: g(α) = kt. In this relationship, g(α) represents the integral model of the reaction, and k is the reaction rate constant. Equation (3) provides a simplified representation of the overall reaction rate, expressing it in terms of the reaction rate constant (k) and the integral model of the reaction (g(α)), obtained by integrating the overall reaction rate with respect to time.

$$g(\alpha) = kt \tag{3}$$

Where k is the reaction rate constant, and g(α) is the integral model of the reaction. Table 2 lists some important reaction models based on different f(α) and g(α). Under non-isothermal reaction conditions and describing the constant kinetic k(T) by Arnious equation once equations (1) and (3) are explained based on equations (4) and (5):

$$\frac{d\alpha}{dt} = \frac{A}{\beta} \times e^{\frac{-E}{RT}} \times F(\alpha) \tag{4}$$

$$g(\alpha) = A \times e^{\frac{-E}{RT}} \times t \tag{5}$$

where β is the heating rate (β = dT/dt). Equation (6) is an integration of equations (4) and (5):

$$g(\alpha) = \frac{A}{\beta} \int_0^T e^{\frac{-E}{RT}} dT \tag{6}$$

If considering the x = E/RT once the equation (6) becomes:

$$g(\alpha) = \frac{AE}{RT} \int_0^{\bowtie} \frac{e^{-x}}{x^2} dx \tag{7}$$

It can be rewritten:

$$g(\alpha) = \frac{AE}{RT} L(x) \tag{8}$$

Where L(x) is an exponential integral and does not have an analytical solution, but there are some numerical estimates. The model-fitting and model-free methods are the main non-isothermal approaches to obtaining the kinetic parameters. The model-fitting method includes fitting different models to α vs temperature curves and concurrently defining E and A parameters. Coats and Redfern method is one of the most common models for model-fitting methods [11], and it uses asymptotic series expansion, which is explained by equation (9):

$$\ln \frac{g(\alpha)}{T^2} = \ln \left[\frac{AR}{\beta E} \left(1 - \frac{2RT^m}{E} \right) \right] - \frac{E}{RT} \tag{9}$$

Where, T^m is mean temperature.

3. Results

The experimental data given in Table 1 were used to obtain the values of E and A corresponding to Equation (9) by plotting ln g(α)/T² versus 1/T and calculating the slope and intercept. Figure 2 shows the ln g(α)/T² versus 1/T for different reaction model-fitting, which are listed in Table 2. Table 3 provides the values of E and A for each reaction based on the different reactions obtained from Figure 2.

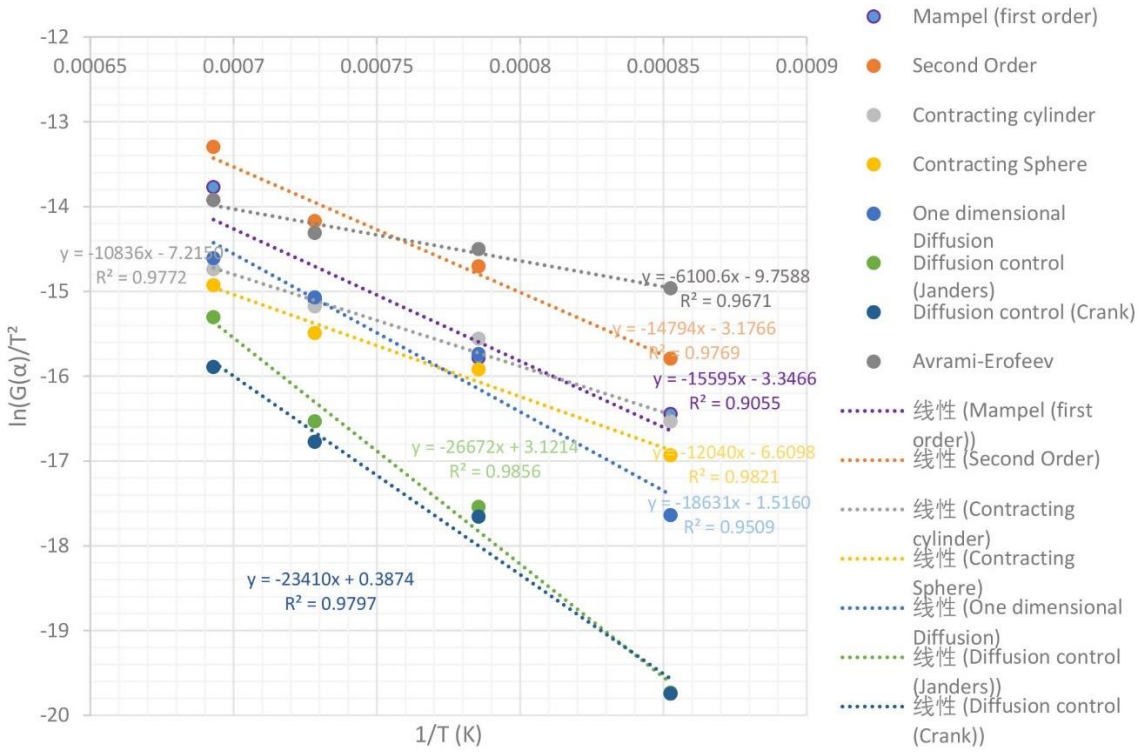

Figure 2 $\ln\frac{g(\alpha)}{T^2}$ vc 1/T for different reaction model-fitting at 900 to 1150°C and atmospheric pressure.

Table 3 The value of E and A for each reaction based on different reaction fitting at 900 to 1150°C and atmospheric pressure.

		E/R	*E (kJ/mol)*	*A (mol/m^3·s)*	*R²*
1	Diffusion control (Crank)	23410	194630.74	3191046.257	0.979
2	Diffusion control (Janders)	26672	221751.01	55913166.43	0.985
3	One dimensional Diffusion	18631	154898.13	384816.9247	0.950
4	Contracting Sphere	12040	100100.56	832.0816389	0.982
5	Contracting cylinder	10836	90090.50	1364.536438	0.977
6	Mampel (first order)	15595	129656.83	53244.32312	0.905
7	Second Order	14794	122997.32	61692.51026	0.976
8	Avrami-Erofeev	6100	50715.40	32.91685679	0.976

The accuracy of each model (R^2) was obtained by comparing the predictable results of each model (using data in Table 3) with the experimental results obtained in tests. Figure 3 compares the ln $g(\alpha)/T^2$ value for each model listed in Table 3 with experimental data.

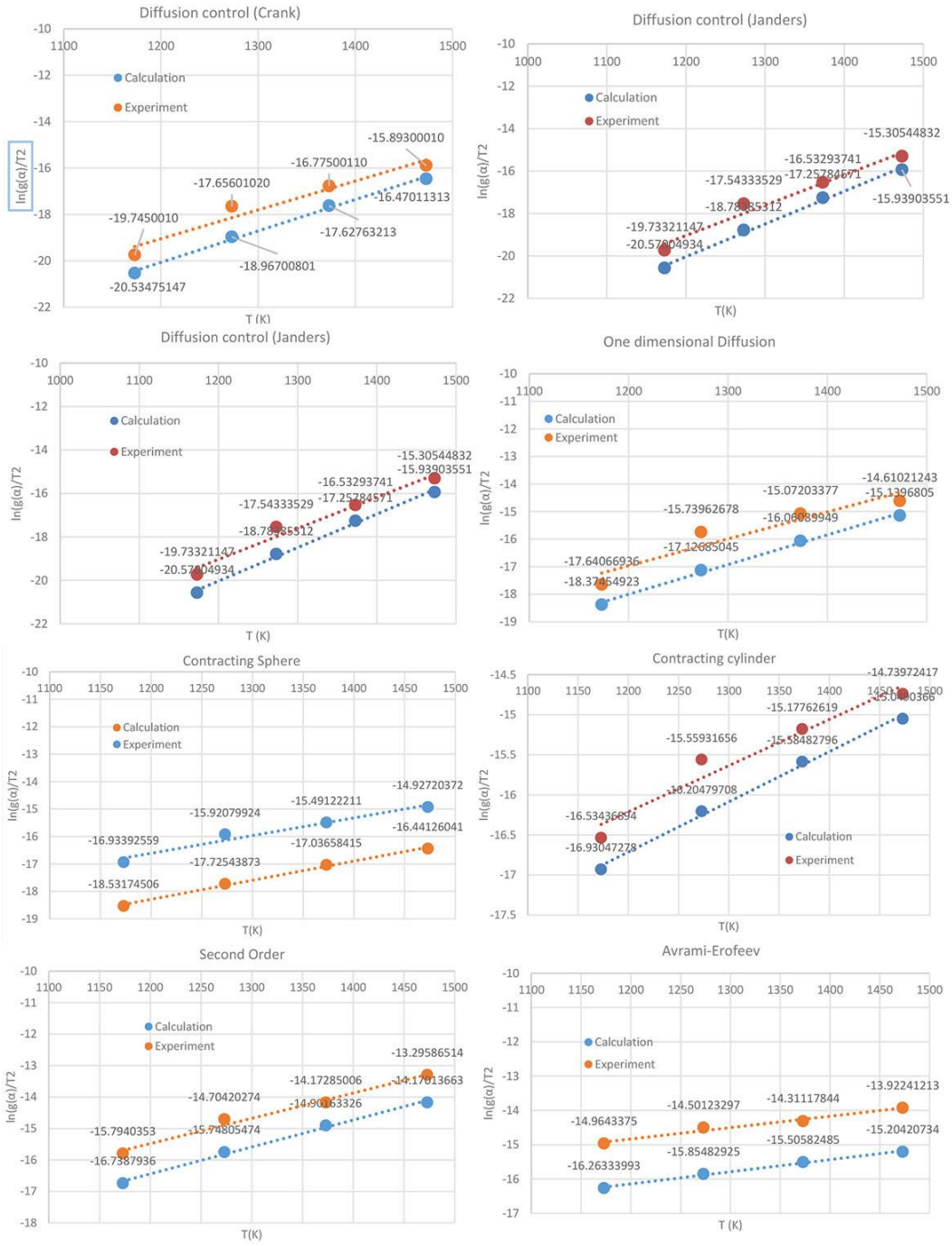

Figure 3 $\ln\frac{\mathbf{g(\alpha)}}{\mathbf{T^2}}$ Versus 1/T by the data obtained in the experiments and the calculated data in Table 3 at 900 to 1150°C for different reaction model-fitting.

Table 4 provides the average error and actual error for the rate models at different temperatures. The lowest error was observed for the contracting cylinder model with about 2.8%, followed by diffusion control (Janders) with 4.95% and diffusion control (Crank) with 5.03%.

Table 4 The average error and the actual error for the rate models at different temperatures.

No.	Model	Actual error at different Temperature K				Average error
		1173	1273	1373	1473	
1	Diffusion control (Crank)	3.99768	7.42138	5.08253	3.62954	**5.03**
2	Diffusion control (Janders)	4.24076	7.07116	4.384631	4.13962	**4.95**
3	One dimensional Diffusion	4.16016	8.81357	6.560931	3.62396	**5.79**
4	Contracting Sphere	9.43561	11.3351	9.975727	10.1429	**10.22**
5	Contracting cylinder	2.39564	4.14851	2.682908	2.09849	**2.83**
6	Mampel (first order)	7.08478	4.97200	3.846526	8.22475	**6.03**
7	Second Order	5.98174	7.09900	5.142108	6.57551	**6.19**
8	Avrami-Erofeev	8.68065	9.33435	8.347645	9.20670	**8.89**

Using the contracting cylinder model, Equation 9 was rewritten as Equation 10, which can be used for a temperature range of 900 to 1170°C with a high approximation.

With the help of COMSOL Multiphysics software, the experimental reactor used in this research was modeled using Equation 10. The average error in this evaluation was less than 3%, demonstrating that the overall reaction rate was governed with acceptable accuracy. Figure 4 provides a comparison of the CFD model results with the experimental results obtained at different temperatures and feed rates up to 2.5 lit/min.

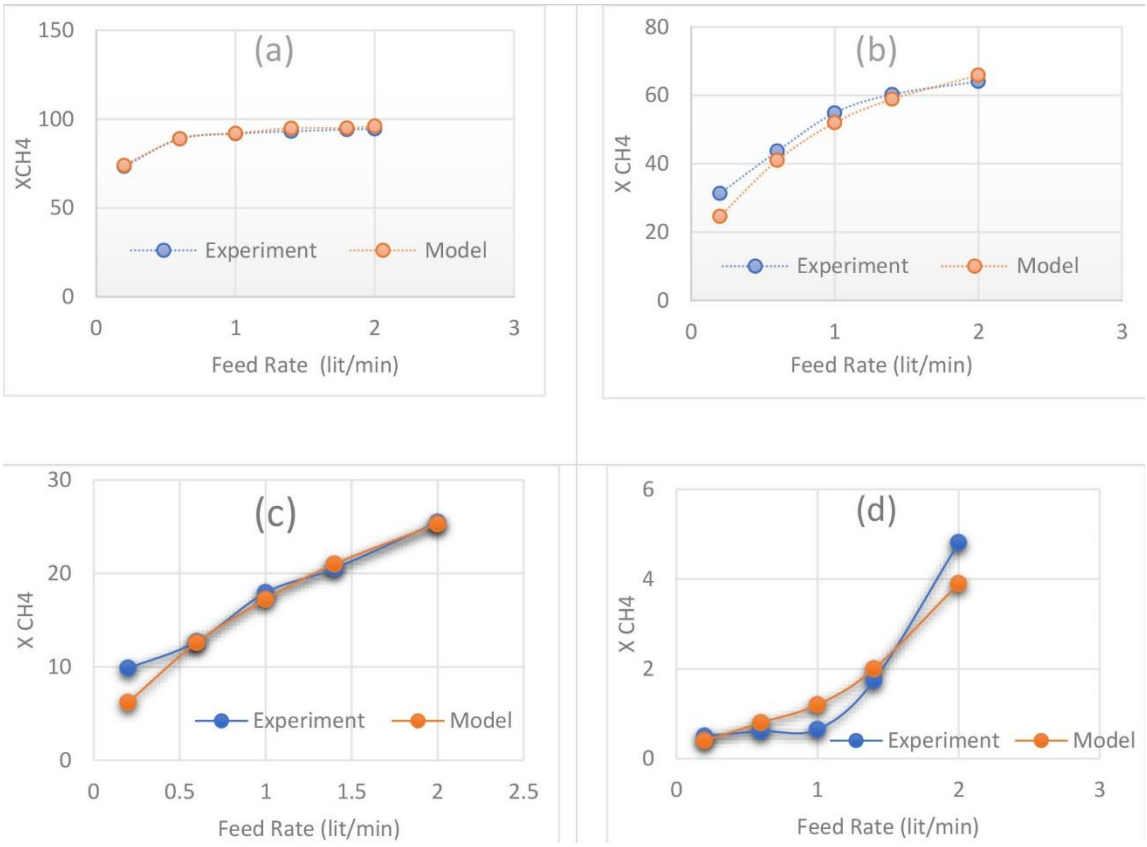

Figure 4 Comparison of CFD model results with experimental results obtained at (a) 850°C, (b) 950°C, (c) 1050°C and (d) 1150°C and feed rates up to 2.5 lit/min.

Using the experimental data given in Table 2, the values of E and A corresponding to equation 9 are obtained by plotting $ln\frac{g(\alpha)}{T^2}$ Versus 1/T the (slope and intercept). Figure 2 indicates the $ln\frac{g(\alpha)}{T^2}$ vs 1/T for different reaction model-fitting, which are listed in Table 2.

Table 3 indicates the value of E and A for each reaction based on the different reactions obtained from Figure 2.

The accuracy of each model (R^2) is obtained by comparing the predictable results of each model (using data in Table 3) with the experimental results obtained in tests. Figure 3 compares the $ln\frac{g(\alpha)}{T^2}$ value for each model listed in Table 3 with experimental data.

The average and actual errors at different temperatures for each model have been given in Table 4. As seen, the lowest error is for the contracting cylinder model with about 2.8%, followed by diffusion control (Janders) with 4.95% and diffusion control (Crank) with 5.03%.

By selecting the Contracting cylinder model, Equation (9) can be rewritten as the following equation, which can be used for a temperature range of 900 to 1170°C with a very high approximation.

$$\ln\frac{2(1-\alpha)^{0.5}}{T^2} = \ln\left[\frac{0.094}{\beta}\right] - \frac{10835.9}{T} \quad (10)$$

Using Equation (10), the condition of the experimental reactor (used in this research) is modelled with the help of COMSOL Multiphysics software to compare and have a more in-depth study.

In this model the test reactor dimention is modeled for simplification in explaining the physical process, mass transfer, heat and momentum. The geometry of the reactor is a cylinder that is symmetrical in terms of geometry and operating conditions, to reduce the volume and time of calculations, the reactor is simulated in two symmetrical dimensions. The thermal cracking reaction takes place in the gas phase, and the solid carbon is deposited on the ceramics. The reactor voidage changes depending on the amount of produced carbon. An ODE[1] physics is coupled to see changes in voidage due to carbon production as a function of time.

The average error in this evaluation is less than 3%. It confidently shows that the overall reaction rate is governed with acceptable accuracy.

4. Discussion

Most previous research focused on the mechanism of intermediate reactions and materials. For instants, Holmen et al. [13] described a model for the production and consumption of the main hydrocarbons at both high and low conversion rates of CH_4 in the temperature range of 1196-1450°C. All of them led to some general MTC reaction rates. The point here is that they can mostly not be used in an unstable reactor because the rate calculations are valid to use in an isothermal condition. While the nature of most industrial reactors is that the gas temperature varies throughout the reactor, and the reaction occurs when the feed gas is warming up inside the reactor. The point is that many researchers have not paid much attention to it, which led to the obtained rates being only used in a limited temperature range. For example, Wullenkord et al. [14]

[1] The Open Dynamics Engine (ODE) is a physics engine and is used for simulating the dynamic interactions between bodies in space.

tried to investigate the conversion rate of methane at 1200 to 1600°C, and Kevorkian et al. [15] investigated the conversion rate of methane at 1383 to 1692°C.

Notably, the thermal decomposition reaction of methane above 850°C is significant, cannot be ignored, and should be considered in a non-isothermal condition. A more detailed study of the conditions governing the reactor by CFD modelling reveals that the reaction rate will change when methane gas reaches the reactor temperature. Afterwards, the reaction is conducted isothermally. Since the reaction rate at the beginning of the reactor and before the methane temperature reached the reactor temperature was much higher than the next stage (isothermal), it is necessary to obtain the overall reaction rate covering both stages.

A detailed analysis of the results obtained from the investigation of thermal methane cracking (TMC) under non-isothermal conditions. To achieve the objective, various kinetic models, including the Contracting Cylinder model, Coats and Redfern model, and others, were used to calculate the reaction rate in non-isothermal conditions. Each model's predictions were compared with the corresponding experimental data, enabling a comprehensive analysis of their performance.

The Contracting Cylinder model exhibited the best fit to the experimental data, with a remarkable error margin of less than ±2.8%. This result demonstrates the model's superior ability to capture the complex behavior of the methane thermal cracking reaction under non-isothermal conditions. In contrast, the other models displayed larger deviations from the experimental data, highlighting their limitations in accurately describing the kinetics of the reaction in industrial reactor settings. The comprehensive analysis of these models has provided valuable insights into their applicability and the significance of considering non-isothermal conditions. The comparison of model predictions with experimental data holds paramount importance as it validates the accuracy and reliability of each kinetic model under real-world conditions. Using non-isothermal models addresses a crucial aspect of the practical application of thermal methane cracking for hydrogen production.

The findings allow us to confidently assess the most suitable kinetic model for industrial-scale reactors, where non-isothermal temperature profiles are the norm. The Contracting Cylinder model's success in predicting the conversion rates of methane to hydrogen and carbon in a non-isothermal environment signifies its potential to enhance reactor design and optimise hydrogen production efficiency.

In conclusion, the comprehensive analysis presented in this section highlights the significance of adopting non-isothermal models to accurately represent the behavior of thermal methane cracking under industrial reactor conditions. The superiority of the Contracting Cylinder model underscores its potential for practical application and advances our understanding of the complex kinetics involved in this process. This study bridges the knowledge gap and paves the way for efficient hydrogen production in industrial and semi-industrial settings.

5. Conclusions

In conclusion, this research aimed to obtain the overall reaction rate of thermal methane cracking (TMC) under non-isothermal conditions covering the temperature range of 850-1200°C. The Coats and Redfern method was used to calculate the reaction rate in non-isothermal conditions, and the Contracting Cylinder model was found to be the most accurate with less than ±2.8% error. This study provides a valuable contribution to the understanding of TMC under non-

isothermal conditions and lays the foundation for developing more efficient industrial reactors for methane cracking.

Acknowledgments

The authors would like to acknowledge the financial support provided by the University of Newcastle, Australia, for the work presented in this paper.

Author Contributions

Dr Mahdi Yousefi played a pivotal role in the research process and served as the primary author responsible for drafting the paper. He conducted the research within the framework of the project titled "A Novel Fuel Converter for the Production of Hydrogen from Natural Gas" at the University of Newcastle (UON). Professor Scott Donne made significant contributions as the principal supervisor of the research, providing valuable guidance and expertise throughout the study. Dr Shabnam Bahremand Abrasi contributed to the research by handling data analysis, formatting, and proofreading tasks, ensuring the accuracy and clarity of the manuscript. Engineer Mohammad Yousefi also played a crucial role in this research, particularly in assisting with the computational fluid dynamics (CFD) modelling, which was essential for the study's methodology. Collectively, these contributions from the authors ensured the successful completion of the research project and the preparation of this manuscript.

Competing Interests

The authors have declared that no competing interests exist.

References

1. Yousefi M, Donne S. Technical challenges for developing thermal methane cracking in small or medium scales to produce pure hydrogen-A review. Int J Hydrogen Energy. 2022; 47: 699-727.
2. Ashik UP, Daud WW, Abbas HF. Production of greenhouse gas free hydrogen by thermocatalytic decomposition of methane-A review. Renew Sustain Energy Rev. 2015; 44: 221-256.
3. Li Y, Li D, Wang G. Methane decomposition to CO_x-free hydrogen and nano-carbon material on group 8-10 base metal catalysts: A review. Catal Today. 2011; 162: 1-48.
4. Yousefi M, Donne S. Experimental study for thermal methane cracking reaction to generate very pure hydrogen in small or medium scales by using regenerative reactor. Front Energy Res. 2022; 10: 971383.
5. Chen CJ, Back MH, Back RA. Mechanism of the thermal decomposition of methane. Washington, USA: ACS Publications; 1976.
6. Serrano DP, Botas JA, Guil Lopez R. H_2 production from methane pyrolysis over commercial carbon catalysts: Kinetic and deactivation study. Int J Hydrogen Energy. 2009; 34: 4488-4494.
7. Holmen A, Olsvik O, Rokstad OA. Pyrolysis of natural gas: Chemistry and process concepts. Fuel Process Technol. 1995; 42: 249-267.
8. Wullenkord M. Determination of kinetic parameters of the thermal dissociation of methane. Aachen, Germany: Universitätsbibliothek RWTH Aachen; 2011.

9. Lee KK, Han GY, Yoon KJ, Lee BK. Thermocatalytic hydrogen production from the methane in a fluidized bed with activated carbon catalyst. Catal Today. 2004; 93: 81-86.
10. Trommer DH, Hirsch D, Steinfeld A. Kinetic investigation of the thermal decomposition of CH_4 by direct irradiation of a vortex-flow laden with carbon particles. Int J Hydrogen Energy. 2004; 29: 627-633.
11. EBRAHIMI KR, Abbasi MH, Saidi A. Model-fitting approach to kinetic analysis of non-isothermal oxidation of molybdenite. Iran J Chem Chem Eng. 2007; 26: 2.
12. Rodat S, Abanades S, Coulié J, Flamant G. Kinetic modelling of methane decomposition in a tubular solar reactor. Chem Eng J. 2009; 146: 120-127.
13. Bilgen E, Galindo J. High temperature solar reactors for hydrogen production. Int J Hydrogen Energy. 1981; 6: 139-152.
14. Wullenkord M, Funken KH, Sattler C, Pitz Paal R. Hydrogen production by thermal cracking of methane-investigation of reaction conditions. Cologne, Germany: DLR; 2010.
15. Kevorkian V, Heath CE, Boudart M. The decomposition of methane in shock waves[1]. J Phys Chem. 1960; 64: 964-968.